Nano LIFE
Vol. 3, No. 4 (2013) 1343006 (10 pages)

DOI: 10.1142/S179398441343006X

DUAL SURFACE-FUNCTIONALIZED SUPERPARAMAGNETIC JANUS NANOCOMPOSITES OF POLYSTYRENE/ Fe_3O_4@SiO_2 VIA A ONE-POT MINIEMULSION METHOD

FENG WANG*, YILONG WANG† and DONGLU SHI*,†,‡
*The Materials Science and Engineering Program
Department of Mechanical and Materials Engineering
College of Engineering & Applied Science, University of Cincinnati
Cincinnati OH 45221-0012, USA

†The Institute for Biomedical Engineering & Nano Science
Tongji University School of Medicine Shanghai 200092, P. R. China
‡shid@ucmail.uc.edu

Received 23 October 2013
Accepted 23 October 2013
Published 6 December 2013

We report a straightforward synthesis of superparamagnetic Janus Polystyrene/Fe_3O_4@Silica ternary nanocomposites via a one-pot miniemulsion approach. The nanocomposites are dual functionalized simultaneously on the same physical carrier, with the carboxyl groups on the polystyrene surface while the silica region is functionalized with silano. With such a unique dual surface structure, it is possible to selectively functionalize multiple surfaces of a single carrier nanoparticle. Multifunctionality can be more readily achieved by this approach for biomedical applications. In this experiment, Doxorubicin is loaded on the silica region, as the model drug, for controlled release via a pH-responsive triggering mechanism. Meanwhile, the polystyrene surface is available for conjugating cancer-specific markers, which is needed for cell targeting. Also discussed are the reaction mechanisms and the key processing parameters in the synthesis of Polystyrene/Fe_3O_4@Silica nanocomposites.

Keywords: Janus; dual-functionalization; miniemulsion.

1. Introduction

In the development of nanocarrier systems for medical diagnosis and treatment, extensive attempts have been made to assemble various components in a structurally and chemically coherent fashion. These components include quantum dots, iron oxides, carbon nanotubes, silica, graphene and polymeric nanomaterials.[1] Surface functionalization is another critical step in the assembly of the complete nanocarrier systems. The nanocarrier is normally conjugated with the biological molecules such as peptide,[2] antibodies,[3] DNA[4] and RNA.[5] For therapy and diagnosis, drugs[6] and imaging agents (quantum dots[7] and dyes[8]) are also incorporated into the carrier system. However, one of the critical issues in nanomedicine deals with multiple surface functionalization on the nanocarriers. As it is well known, most of the nanocarriers are symmetrical with only one

surface, but required to carry several major components in medical diagnosis and treatment. These include fluorescent materials for optical imaging, magnetic particles for separation, bio markers for cell targeting and anti-cancer drug loading for therapy. As such, a single surface nanoparticle system is quite limited in the assembly of all aforementioned components for simultaneous medical therapy and diagnosis. A new terminology, "theranostics," has been suggested particularly useful for this multifunctional system. Multifunctional conjugates on a single surface carrier may also interact with each other, both chemically and structurally, leading to adverse effects. It is, therefore, critical to develop multiple-surface nanostructures for assembly of all required constitutions in a clinically viable delivery system.

Janus nanoparticles are anisotropic in shape, composition and surface chemistry.[9] The characteristic asymmetry makes them ideal candidates for multicomponent conjugation.[10] Specific moieties can be conjugated selectively onto the functionally distinct surfaces of a Janus particle for diagnostic or therapeutic purposes.[11,12] Recently there have been several reports[13–16] on the design and synthesis of the "truly multifunctional entities".[17] However, most of the approaches involve complex reaction steps which limit the controllability.

In this study, superparamagnetic Janus nanocomposites (SJNCs) of polystyrene/Fe_3O_4@SiO_2 were fabricated via a combined process of miniemulsion polymerization and solgel reaction.[18] The ternary SJNCs are composed of a polystyrene (PS) core and a half shell of silica with iron oxide (Fe_3O_4) nanoparticles embedded in its matrix. As shown in Fig. 1, the PS surface is decorated with the carboxyl groups while the silica surface is conjugated with the silano groups. The Janus structure is therefore rendered dual functional, ideally suited for selective chemical modification. To test the surface functionality of SJNCs, doxorubicin (DOX) was conjugated onto the silica shell and release profiles were recorded *in vitro*.

2. Methods

2.1. *Materials and chemicals*

Ferric chloride hexahydrate ($FeCl_3 \cdot 6H_2O$), ferrous chloride tetrahydrate ($FeCl_2 \cdot 4H_2O$), oleic acid (OA), styrene (St), tetraethoxysilane (TEOS), sodium dodecyl sulfate (SDS), hexadecane (HD) and 4,4'-azobis(4-cyanovaleric acid) (ACVA) were purchased from Sigma-Aldrich (USA). Ammonium hydroxide (NH_4OH, 29.79 wt.%), hydrofluoric acid (HF), toluene, 1-Ethyl-3-(3-dimethylaminopropyl), carbodiimide HCl (EDC), N-Hydroxysuccinimide (NHS) and phosphate buffered saline (PBS) were purchased from Fisher Scientific (USA). 3-(triethoxysilyl)propyl isocyanat, adipic acid dihydrazide, trifluoroacetic acid (TFA) were purchased from Sigma-Aldrich (USA) Doxorubicin hydrochloride (DOX) was purchased from Meiji Seika Kaisha, Ltd. (Tokyo, Japan). Acetate buffer solutions (10 mM) were prepared in our laboratory. Styrene monomer was washed with 5 wt.% sodium hydroxide solution and stored at −20°C before use. All other chemicals were used as received. Deionized (DI) water was used for the entire experiment. Ultra

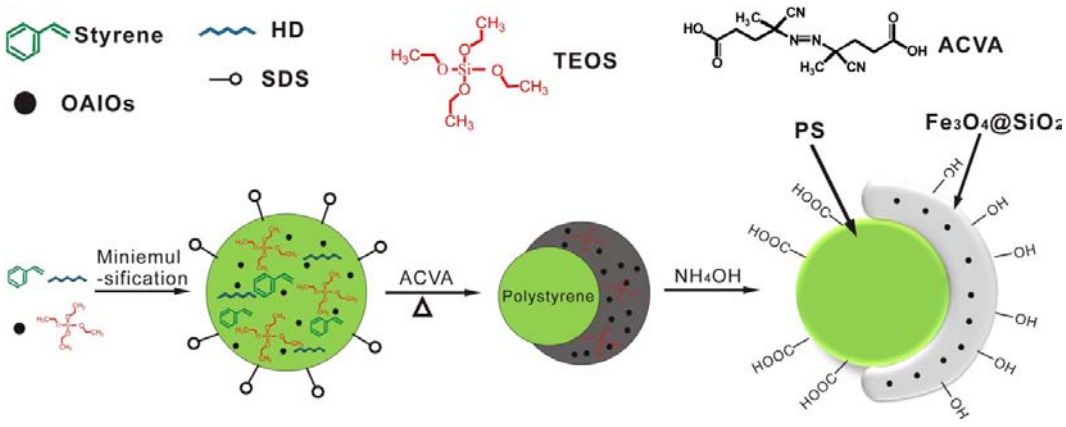

Fig. 1. Schematic illustration showing the formation of polystyrene/Fe_3O_4@silica superparamagnetic Janus nanocomposites (SJNCs).

high purity nitrogen gas was obtained from Wright Brother Gas.

2.2. *Methods*

2.2.1. *Synthesis of oleic acid-functionalized iron oxide nanoparticles*

Oleic acid surface-functionalized iron oxide nanoparticles (∼10 nm) (OAIOs) were fabricated using a method previously reported.[18] In a typical reaction, $FeCl_2 \cdot 4H_2O$ (7.72 g) and $FeCl_3 \cdot 6H_2O$ (24 g) were dissolved in 100 mL of DI water and kept at 80°C with nitrogen bubbling for 0.5 h, followed by addition of NH_4OH (50 g). Oleic acid (3.76 g) was then added and the dispersion was kept at 80°C for another 3 h. After cooling down to room temperature, the precipitates OAIOs were washed with ethanol and DI water, dispersed in octane and dried by rotary evaporation.

2.2.2. *Synthesis of polystyrene/Fe_3O_4@SiO_2 SJNCs*

SJNCs were synthesized using a miniemulsion process similar to the method we reported earlier.[19] The water phase was prepared by dissolving 0.092 g of SDS in 39 g of DI water. The oil phase was formed by dissolving 25 mg of OAIOs, 0.4 g of HD and 2 g of TEOS in 8 g of St monomers. The oil phase was then injected dropwise into the water phase under powerful sonication, followed by mechanical stirring at 250 rpm for 0.5 h. The miniemulsion droplets were formed by sonicating the emulsions for 10 min at 500 W at a duty cycle of 50% using a Scientz-IID sonifier (Ningbo, China) in an ice bath. The miniemulsion mixture was subsequently transferred to a three-headed flask. Upon adding 0.12 g of ACVA [neutralized by 1 mL of NaOH solution (0.856 M)] into the flask, the system was deoxygenized with nitrogen bubbling for 0.5 h with 250 rpm mechanical stirring. The flask was moved into the 80°C water bath with a condenser under nitrogen protection to start St monomer polymerization. After 60 min, 50 uL of NH_4OH was introduced to the reaction. For another 5 h, the reaction system was removed from the water bath and stirred at room temperature overnight. Finally, SJNCs were purified by washing with DI water using an external magnetic field and dried under vacuum at room temperature. Schematic drawing of the reaction process is illustrated in Fig. 1.

2.2.3. *DOX loading on SJNCs and evaluation of pH sensitivity*

About 52.26 mg of adipic acid dihydrazide was dissolved in 4 mL of DMSO. Then 74.2 uL of 3-(Triethoxysilyl)propyl isocyanat was dissolved in 500 uL of DMSO and added into the adipic acid dihydrazide solution dropwise under vigorous stirring. After reaction overnight, DMSO was removed under reduced pressure at 80°C and the waxy residue was dissolved in 2 mL of EtOH.

A standard silane coupling method was employed to modify the silica surface. About 40 mg of SJNCs was dispersed in 16 mL of EtOH/H_2O (95:5) mixture. The 60 uL of the above silane-hydrazide solution in EtOH was added into the SJNCs dispersion under stirring. The pH was set at 5 by HCl and the dispersion was stirred for 4 h at room temperature. The pH was then adjusted to neutral by adding NaOH and stirred overnight. The surface-modified SJNCs–$NHNH_2$ were washed by magnetic separation with EtOH and DI water and dried at room temperature under vacuum for drug loading.

DOX was conjugated to the surface of silica half shell through the formation of hydrazone bonds. Briefly, 35 mg of SJNCs–$NHNH_2$ nanocomposites were dispersed in 15 mL of DOX solution in anhydrous methanol (0.33 mg mL^{-1}) and 3 uL of TFA was added to reach the pH of 5. The mixture was stirred in darkness for 40 h at room temperature and intense magnetic wash with anhydrous methanol was carried out till no absorbance at 480 nm was detected in the supernatant on a UV-Vis spectrophotometer. The SJNCs–DOX conjugates were dried at room temperature under vacuum.

2.3. *Characterization*

The SJNCs were dispersed in DI water and dried on the carbon-coated copper grid for TEM examination. TEM images were obtained on a Philips Tecnai 20 transmission electron microscope with an accelerating voltage of 200 kV and a JEOL JEM2010 electron microscope equipped with EDX.

STEM images and elemental mapping were obtained on a Zeiss Ultra55 equipped with Oxford Aztec X-Max 50 EDS system operated at an accelerating voltage of 1 kV.

Size distribution of SJNCs dispersed in DI water was measured using a Malvern Zetasizer (Nano ZS).

The SJNCs were pelleted with potassium bromide powder and infrared spectroscopy was obtained using a transmission method on a Nicolete 6700 FTIR from Thermo Scientific.

UV-Vis spectra of hydrazide-modified and DOX-loaded nanocomposites were recorded on a Hitachi U-3000 spectrophotometer using a cuvette with the path length of 1 cm and nominal volume of 350 uL.

The samples were etched with hydrofluoric acid. The Janus nanocomposites were dispersed in 5% HF solution in DI water and rotated overnight. The products were collected with a centrifuge at 12 000 rpm after dialysis in DI water in a dialysis bag with the cutoff of 3000 Da. For samples etched with toluene, the Janus nanocomposites were dispersed in toluene and rotated overnight. The products were magnetically washed five times with DI water.

The magnetic properties were measured at room temperature using a vibrating sample magnetometer (VSM 7407, Lake Shore, USA).

3. Results and Discussion

3.1. *Morphology and composition*

3.1.1. *Microscopy observation*

The SJNCs were subjected to TEM and STEM/EDS examination. Figure 2(a) shows a clear image of the OAIOs with a typical dimension of 9 nm. As can be seen in Fig. 2(b), the SJNCs are structured with a core covered by a half shell of the nanoparticles embedded in the matrix. The SJNCs are estimated to be on the order of 300 nm, with a PS core of about 200 nm, and a hybrid shell of 100-nm thick. This is consistent with the DLS data [see Fig. 2(d)], which show an average size of 313 nm with a polydispersity index (PDI) of 0.090. The size distribution is quite narrow showing very low polydispersity. As shown in the EDS spectra [see Fig. 2(c)], the signals from the core are mainly associated with C and O, with minor ones of Si and Fe, indicating a hybrid shell structure at the back of the core. On the other hand,

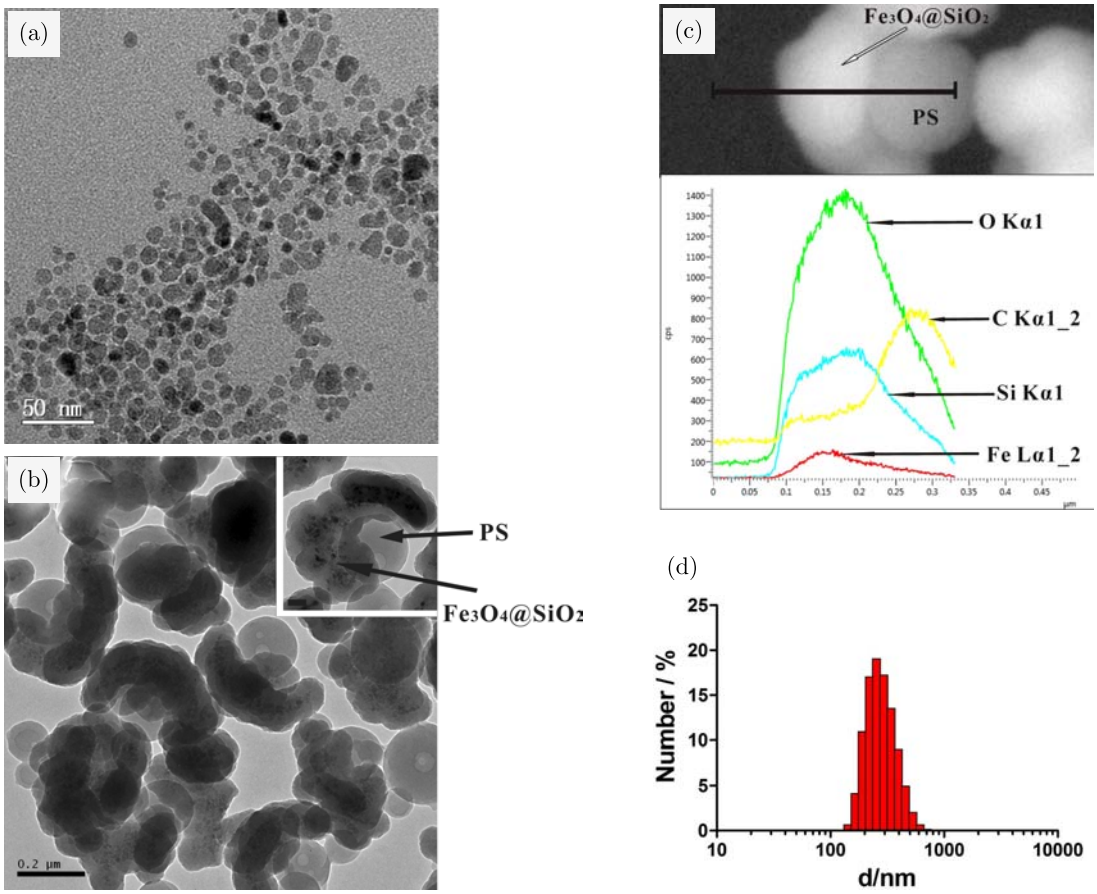

Fig. 2. TEM images of (a) oleic acid-modified Fe_3O_4 nanoparticles (OAIOs) (scale bar denotes 50 nm); (b) the dual-functionalized polystyrene/Fe_3O_4@silica Janus nanocomposites, the scale bar is 200 nm (inset image is the magnified image of one nanocomposite particle, scale bar is 50 nm; (c) Elemental mapping of an individual SJNC and (d) DLS data of SJNCs in DI water.

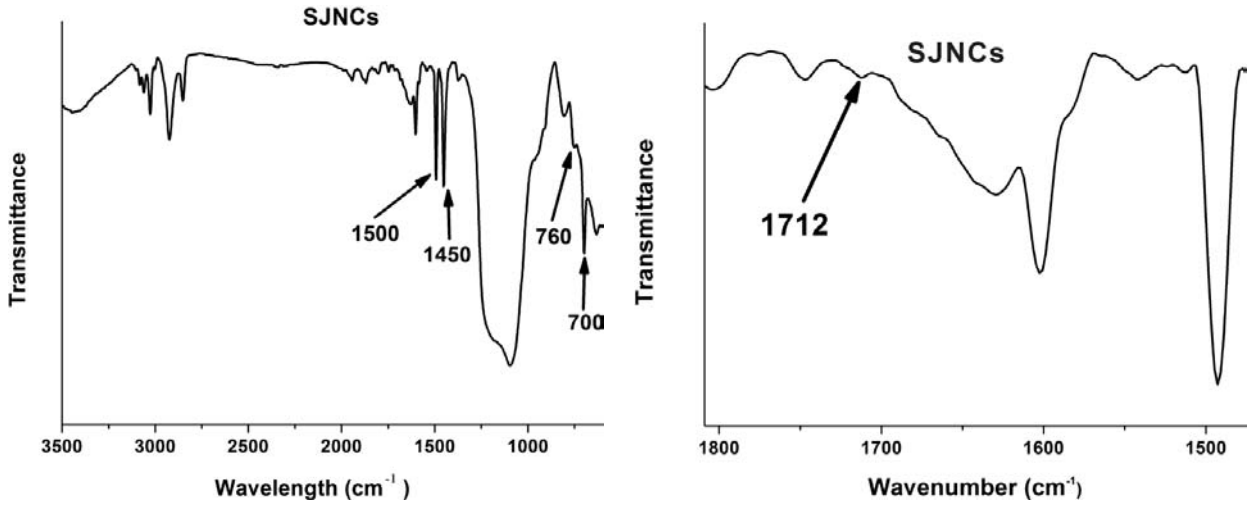

Fig. 3. (a) FTIR spectra of Polystyrene/Fe_3O_4@Silica Janus nanocomposites and (b) magnified area (1450–1800 cm^{-1}) of spectra (A).

there are much stronger signals of Si and Fe from the shell, compared to the spectra of the core. These results suggest a core–shell structure of SJNCs. The system is composed of a pure polymer core, (polystyrene in this case), and a silica half shell with iron oxide nanoparticles embedded in its matrix. These experimental results on the basic structure of SJNCs are consistent with our earlier study.[19]

3.1.2. *Chemical structure analysis*

In FTIR spectrum [see Fig. 3(a)], the SJNCs exhibit strong peaks from the silica vibrations in the range of 800–1250 cm^{-1}, while the peaks at 2850 cm^{-1} and 2920 cm^{-1} represent –CH stretching. The peak at 1712 cm^{-1} [see Fig. 3(b)] can be assigned to carboxyl groups on the PS surface, with its weak intensity due to low quantities. The peaks at 1450 cm^{-1} and 1500 cm^{-1} are attributable to the C=C frame stretching vibration in aromatic ring, while the peaks at 700 cm^{-1} and 760 cm^{-1} are characteristics of the single-replaced phenyl ring.[20,21] It is possible that the SiO_2/Fe_3O_4 hybrid shell attaches to the PS core by forming a covalent –Si–O–C– bond. The peak for this bond at around 1100 cm^{-1} is not observed, however, possibly due to its overlap with the strong signal from silica vibrations in the same range.

3.1.3. *Selective etching*

As shown in Fig. 4(a), only the PS cores are left under TEM observation as silica and Fe_3O_4 nanoparticles are dissolved in HF. The EDX spectrum in Fig. 4(b) shows only carbon as the component of the PS cores. On the other hand, toluene can easily dissolve polystyrene. Only the hybrid shells with black dots inside remain after etching with toluene [see Fig. 4(c)]. The EDX spectrum [see Fig. 4(d)] shows distinctively the silica and iron oxide nanoparticles. These results establish the main chemical structures of SJNCs.

3.1.4. *Magnetic properties*

The magnetic properties of OAIOs and SJNPs were characterized by magnetization measurements at room temperature. As is shown in Fig. 5, both OAIOs and SJNPs exhibit superparamagnetic bahaviors with negligible magnetic remanence. Superparamagentism, as is well known, is one of the required properties for re-dispersion after the removal of the external magnetic field. The superparamagnetism is a key property required for MRI, hyperthermia and magnetic targeting.

3.2. *Reaction mechanism*

The phase separation between the inorganic and organic components is essential for the formation of SJNCs during polymerization followed by sol–gel reaction of TEOS. As illustrated in Fig. 1, the one-pot synthesis process is described as follows: (1) The miniemulsion system is created by miniemulsifying

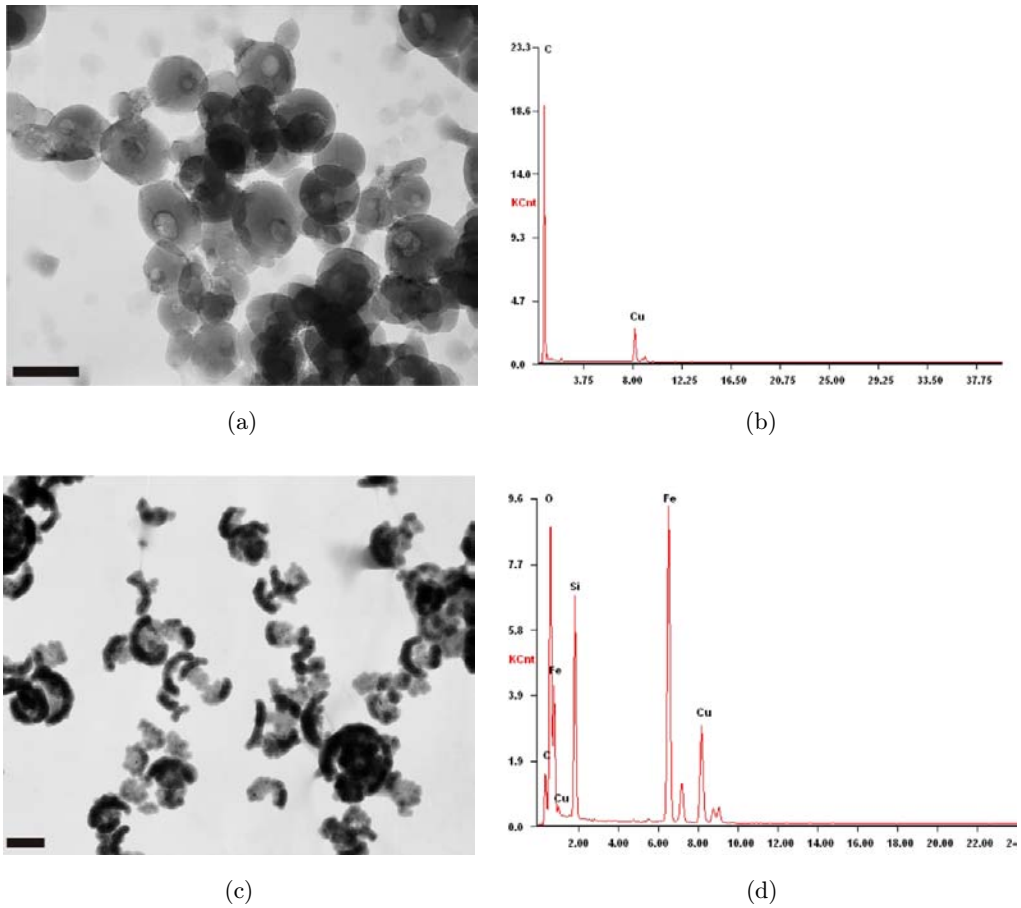

Fig. 4. (a) TEM image of SJNCs after etching with HF; (b) EDX elemental analysis spectra of the particles in (a); (c) TEM image of the SJNCs after toluene etching, and (d) EDX elemental spectra of the shells in (c). The scale bars in both (a) and (c) are 200 nm.

the pre-emulsified mixture of the oil phase and water phase using a sonifier; (2) Polymerization of St monomers occurs inside the droplets. This mechanism is different from conventional emulsion, in which polymerization takes place in the monomer-swelled micelles.[22] In polymerization, St monomers in the miniemulsion droplets gradually transfer into polystyrene chains, which decreases their affinity to other hydrophobic portions.[23] At this intermediate stage, the hydrophobic mixture of

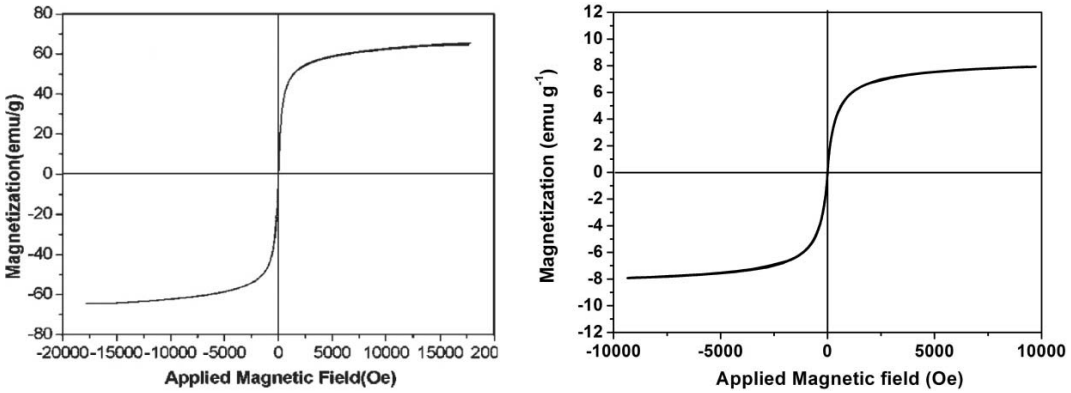

Fig. 5. Magnetization curves of (a) oleic acid-modified iron oxide nanoparticles, and (b) SJNCs at room temperature.

the remaining St monomers (OAIOs and TEOS) is located eccentrically on the PS particle surface. (3) Upon phase separation of other hydrophobic components of the PS particle, NH_4OH is added to initiate the sol–gel reaction of TEOS, in order to generate silica. With addition of NH_4OH, oleic acid on the Fe_3O_4 surface is transformed to oleate,[24] thus significantly lowering the hydrophobicity of OAIOs. As a result, OAIOs tend to be more compatible with TEOS and produce the Fe_3O_4@silica hybrid. The initiator ACVA can introduce the carboxyl groups on the PS particle surface. The reaction takes place with the silanol groups on the silica surface to form –Si–O–C– bond. In this way, the Fe3O4@Silica hybrid tends to grow along the PS particle surface and form a shell. The formation mechanism of the half shell, instead of complete coverage on the PS particle, is still under investigation. It is our hypothesis that the amount of TEOS in the initial formulation is important in the formation of half-shell coverage. If more of TEOS is presented and longer incubation time is allowed, silica may grow along the curvature of the PS core and close-to-full coverage is reasonably expected.

3.3. *Key parameters in synthesis*

There are two key factors for generating the Janus structure:

(1) Formation of miniemulsion system. When the miniemulsion system is developed, all hydrophobic components including St monomers, HD, OAIOs and TEOS are incorporated into the miniemulsion droplets stabilized by the surfactant SDS. The amount of SDS is below the critical micelle concentration (CMC) so that it does not form micelles. Polymerization of St monomers takes place *in situ* in each miniemulsion droplet.[22] Reaction stops simultaneously when the reagents in the droplets are consumed up. This is the major difference between miniemulsion and conventional emulsion.

(2) Phase separation between PS and other hydrophobic portions. The phase separation occurs between OAIOs and polymer. Meanwhile, silica condenses from TEOS, separated from the PS particles, which is critical to the morphology of SJNCs. With the polystyrene chains increasing in length and number, OAIOs and TEOS with the remaining St monomers experience phase separation, but physically intact. After adding NH_4OH, TEOS begins to undergo sol–gel reaction while oleic acid is being converted to oleate ions. This process renders OAIOs hydrophilic, and makes it more compatible with hydrolyzed TEOS.[19] Hydrophilic iron oxide nanoparticles can serve as nucleation sites of silica and facilitate the formation of Fe_3O_4@SiO_2 half shell on the PS particles. The nanoparticle morphology can be modified by changing the starting time of NH_4OH addition. If NH_4OH is added much earlier (10 min after polymerization), the final product is a composite [see Fig. 6(a)] with all components (polystyrene, silica and Fe_3O_4). However, it does not form an asymmetric structure as there is insufficient time for the TEOS/OAIOs mixture to

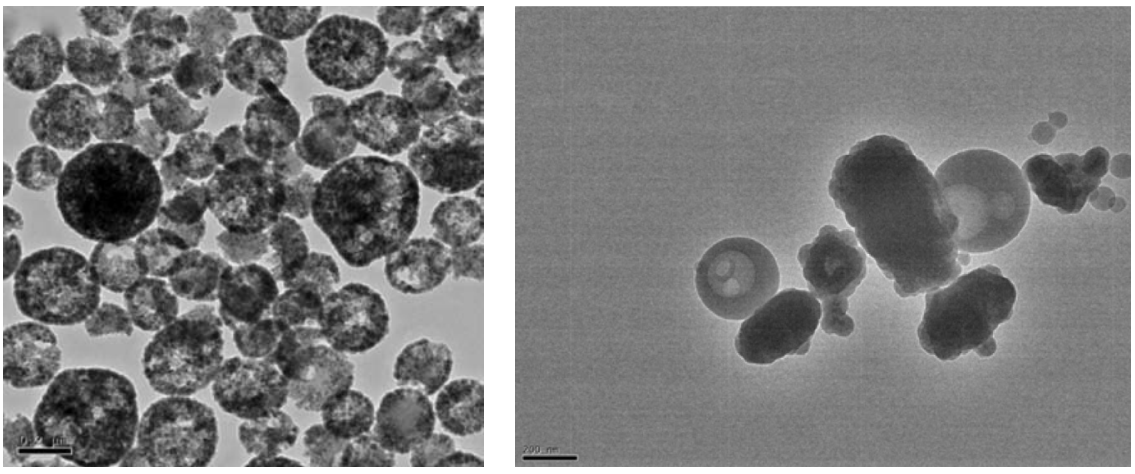

(a) (b)

Fig. 6. TEM images of asymmetric PS/Fe_3O_4@SiO_2 nanocomposites when NH_4OH is added (a) 10 min and (b) 150 min after polymerization of the St monomer at 80°C. Both scale bars denote 200 nm.

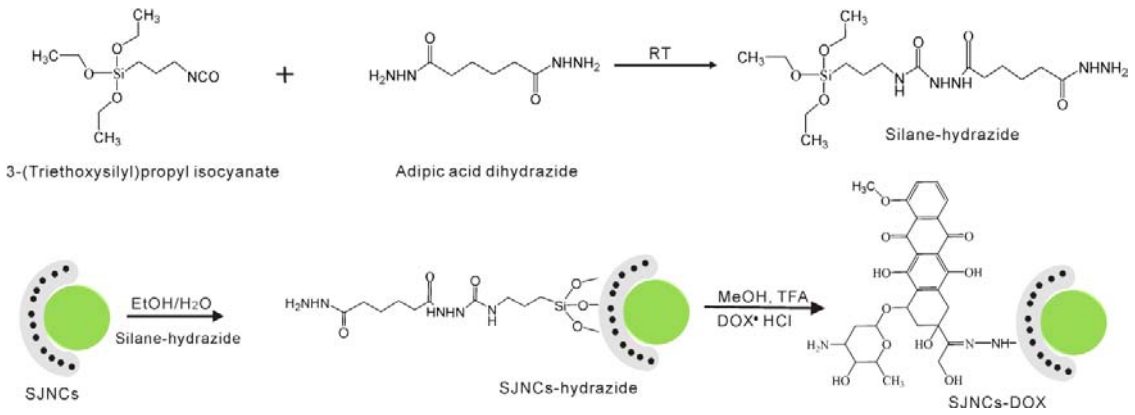

Fig. 7. Schematic drawing of DOX loading onto the Fe_3O_4@silica hybrid shell surface.

be driven away from the polystyrene particles. As aresult, all components are concentrated within the composite particle. In contrast, if NH_4OH is added later, i.e., 150 min after polymerization initiates, the Janus structure is developed [see Fig. 6(b)]. The oval-shaped Fe_3O_4/silica hybrid forms a heterodimer with the PS particle as a half shell. Phase separation between PS and OAIOs/TEOS mixture is already excessive before NH_4OH addition. Under this condition, the silica does not grow along the PS particle curvature. Instead, the hybrid only partially covers a small area of the PS particle as a heterodimer.

3.4. *Drug loading and release assessment*

To investigate the drug loading capability of SJNCs, DOX was conjugated to the silica shell via a hydrazone bond [see Fig. 7]. The hydrazone bond is relatively stable at physiological condition (pH 7.2–7.4) but can hydrolyze at endocytic condition (pH 4.5–6.5). This is an excellent characteristic of the carrier system for well-controlled release of doxorubicin, and in turn the significantly reduced side effects.[25] The drug-loaded SJNCs were characterized by UV-Vis. As is shown in Fig. 8, the spectrum of SJNCs–DOX exhibits a broad shoulder with the peak at 517 nm compared to the hydrazide-modified SJNCs. The shift from the characteristic peak of pure DOX at around 480 nm is likely associated with the covalent bonding formed between DOX and silica surfaces. Similar results were found by Hu *et al.*[26] These results clearly show successful conjugation of DOX to the hybrid shell surface via hydrazone bonding. The DOX loading capacity was

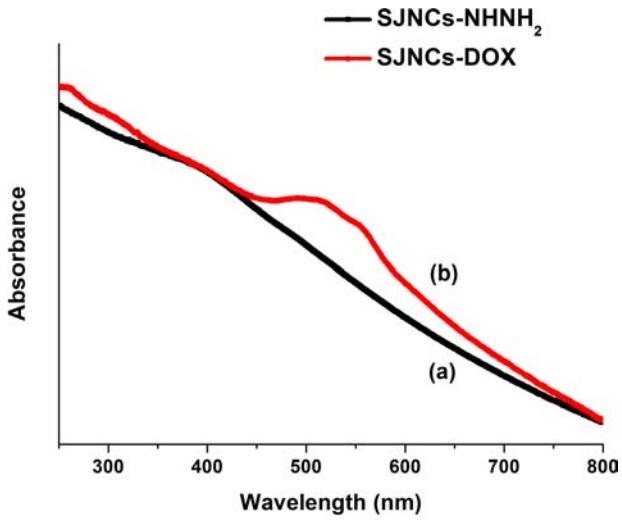

Fig. 8. UV–Vis spectra of (a) SJNCs–$NHNH_2$ and (b) SJNCs–DOX.

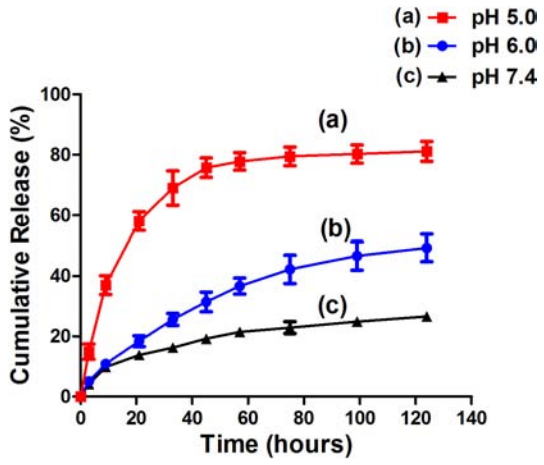

Fig. 9. DOX release profiles from DOX conjugated SJNCs at (a) pH 5.0 and (b) pH 6.0 and (c) pH 7.4.

determined to be 1.75 ± 0.25 wt.% using a subtraction method.

The drug release was investigated in buffer solutions of different pH values. It can be seen in Fig. 9 that at pH 7.4, a simulated physiological condition, accumulative DOX release after 125 h is 26.6%. In contrast, at pH 5.0 and pH 6.0, which are similar to the environment in the endocytic compartments and on tumor sites, DOX releases are much faster and the accumulative release reaches, respectively, 81.1% and 49.3% after 125 h. These results are consistent with the release mechanism that is related to the acid-sensitive nature of hydrazone bonding. As environment becomes more acidic, the increase in H^+ concentration in the buffer solutions accelerates the hydrolysis of hydrazone bond, thus releasing more DOX from the conjugates. However, the drug delivery needs to be targeted at tumor sites. The polystyrene surface of SJNCs is to be utilized for conjugating cancer-specific antibodies. As a next step, we plan to conjugate folic acid to the polystyrene surface as the targeting group via carbodiimide-mediated coupling.

4. Conclusion

Dual-functionalized superparamagnetic Janus Polystyrene/Fe_3O_4@Silica nanocomposites (SJNCs) are synthesized by a straight-forward one-pot miniemulsion method. The SJNCs are found to be superparamagnetic and monodispersed. The Janus nanocomposites are structurally and chemically anisotropic and geometrically asymmetrical. Such a unique structure enables surface functionalization in a multiple fashion, which is highly desirable in the design and development of carrier systems for medical diagnosis and treatment. It is found in this study that phase separation plays a key role in developing the Janus structure. The surface functionality is confirmed by conjugation of doxorubicin via a pH-sensitive hydrazone bond and release behaviors are monitored. The dual surface nature of a single particle makes it an ideal candidate for biomedical applications such as optical imaging, cell targeting, drug delivery, gene transfection and protein purification.

Acknowledgments

This work was supported by National Natural Science Foundation of China (No. 51003077; No. 51173135) Shanghai Nano-program (No. 11nm-0506100) and the Fundamental Research Funds for the Central Universities.

References

1. F. Wang, G. M. Pauletti, J. Wang, J. Zhang, R. C. Ewing, Y. Wang and D. Shi, *Adv. Mater.* **25**, 3485 (2013).
2. I. Ojea-Jimenez, L. Garcia-Fernandez, J. Lorenzo and V. F. Puntes, *ACS Nano* **6**, 7692 (2012).
3. H. S. Cho, Z. Dong, G. M. Pauletti, J. Zhang, H. Xu, H. Gu, L. Wang, R. C. Ewing, C. Huth, F. Wang and D. Shi, *ACS Nano* **4**, 5398 (2010).
4. F. M. Kievit, O. Veiseh, N. Bhattarai, C. Fang, J. W. Gunn, D. Lee, R. G. Ellenbogen, J. M. Olson and M. Q. Zhang, *Adv. Funct. Mater.* **19**, 2244 (2009).
5. G. Liu, J. Xie, F. Zhang, Z. Y. Wang, K. Luo, L. Zhu, Q. M. Quan, G. Niu, S. Lee, H. Ai and X. Y. Chen, *Small* **7**, 3260 (2011).
6. C. H. Lee, S. H. Cheng, I. P. Huang, J. S. Souris, C. S. Yang, C. Y. Mou and L. W. Lo, *Angew. Chem. Int. Ed.* **49**, 8214 (2010).
7. M. N. Rhyner, A. M. Smith, X. H. Gao, H. Mao, L. L. Yang and S. M. Nie, *Nanomedicine* **1**, 209 (2006).
8. S. Santra, C. Kaittanis, J. Grimm and J. M. Perez, *Small* **5**, 1862 (2009).
9. J. Hu, S. X. Zhou, Y. Y. Sun, X. S. Fang and L. M. Wu, *Chem. Soc. Rev.* **41**, 4356 (2012).
10. S. H. Hu and X. Gao, *J. Am. Chem. Soc.* **132**, 7234 (2010).
11. K. H. Roh, M. Yoshida and J. Lahann, *Materialwiss. Werksttech.* **38**, 1008 (2007).
12. C. J. Xu, B. D. Wang and S. H. Sun, *J. Am. Chem. Soc.* **131**, 4216 (2009).
13. Z. F. Li, D. Y. Lee, M. F. Rubner and R. E. Cohen, *Macromolecules* **38**, 7876 (2005).
14. J. R. Howse, R. A. L. Jones, A. J. Ryan, T. Gough, R. Vafabakhsh and R. Golestanian, *Phys. Rev. Lett.* **99**, 048102 (2007).
15. Y. Wang, B. H. Guo, X. Wan, J. Xu, X. Wang and Y. P. Zhang, *Polymer* **50**, 3361 (2009).
16. S. Hwang, K. H. Roh, D. W. Lim, G. Y. Wang, C. Uher and J. Lahann, *Phys. Chem. Chem. Phys.* **12**, 11894 (2010).
17. M. Lattuada and T. A. Hatton, *Nano Today* **6**, 286 (2011).
18. Y. L. Wang, F. Wang, B. D. Chen, H. Xu and D. L. Shi, *Chem. Commun.* **47**, 10350 (2011).
19. Y. L. Wang, H. Xu, Y. S. Ma, F. F. Guo, F. Wang and D. L. Shi, *Langmuir* **27**, 7207 (2011).
20. L. B. Feng, H. Li, M. J. Yang and X. W. Wang, *Colloid. Polym. Sci.* **288**, 673 (2010).

21. K. Zhang, W. Wu, H. Meng, K. Guo and J. F. Chen, *Powder Technol.* **190**, 393 (2009).
22. K. Landfester, *Macromol. Rapid Commun.* **22**, 896 (2001).
23. F. Montagne, O. Mondain-Monval, C. Pichot and A. Elaissari, *J. Polym. Sci. Pol. Chem.* **44**, 2642 (2006).
24. A. K. F. Dyab, M. Ozmen, M. Ersoz and V. N. Paunov, *J. Mater. Chem.* **19**, 3475 (2009).
25. C. H. Lee, S. H. Cheng, I. P. Huang, J. S. Souris, C. S. Yang, C. Y. Mou and L. W. Lo, *Angew. Chem. Int. Ed.* **49**, 8214 (2010).
26. Q. D. Hu, H. Fan, Y. Ping, W. Q. Liang, G. P. Tang and J. Li, *Chem. Commun.* **47**, 5572 (2011).